Engineering Structures 33 (2011) 1894–1907

Contents lists available at ScienceDirect

Engineering Structures

journal homepage: www.elsevier.com/locate/engstruct

Investigation of vortex-induced vibration of a suspension bridge with two separated steel box girders based on field measurements

Hui Li [a,*], Shujin Laima [a], Jinping Ou [a,b], Xuefeng Zhao [b], Wensong Zhou [a], Yan Yu [b], Na Li [c], Zhiqiang Liu [c]

[a] *School of Civil Engineering, Harbin Institute of Technology, Harbin, 150090, China*

[b] *School of Civil and Hydraulic Engineering, Dalian University of Technology, Dalian, 116024, China*

[c] *CCCC Highway Consultants CO., LTD, Beijing, 100088, China*

ARTICLE INFO

Article history:
Received 17 April 2010
Received in revised form
15 February 2011
Accepted 17 February 2011
Available online 1 April 2011

Keywords:
Field measurements
Vortex-induced vibration
Wind pressure
Spatial–temporal maps
Span-wise correlation

ABSTRACT

This paper investigates the vortex-induced vibration of a twin steel box girder suspension bridge with a centre span of 1650 m based on field measurements. Two ultrasonic anemometers, two tri-axial accelerometers and 52 wind pressure sensors are installed at the quarter span section. The other 20 pressure sensors are installed in another 5 sections, and each section has 4 pressure sensors. Four vortex-induced oscillation events are measured. The analytical results indicate that the vortex-induced vibration more likely occurs in a low wind speed range of 6–10 m/s, with the wind direction nearly perpendicular to the bridge line, and low turbulence intensity. The mean pressure distribution on the surface of the bridge deck is obtained and the characteristics of fluctuant pressures are analysed by proper orthogonal decomposition (POD) method. Moreover, the spatial–temporal evolution of flow around the bridge deck is investigated. The results indicate that in the beginning stage of vortex-induced resonance, the regular vortex shedding phenomena occur only in the gap of the deck and at tailing region of downstream deck; however, when in the lock-in stage, the vortex shedding is strengthened due to the dramatic vibration, and the regular vortex shedding phenomena extend to the entire lower surface of downstream deck and the tail of upstream deck, the vortex shedding regions in the gap and lower surface link together. In the lock-in range, the span-wise correlation of the wind pressure is analysed, and the correlations of wind pressure along the bridge line are very high and do not decrease with the increase in distance.

1. Introduction

With increases in the spans of bridges, bridges become more flexible and small damping occurs. Therefore, the bridges more readily oscillate dramatically when subject to wind. The vortex-induced vibration (VIV) is just a typical phenomenon of wind-induced vibration, especially for the long-span bridges. When flow passes through the bridge deck, vortex shedding occurs. If the vortex shedding frequency is close to the natural frequency of the bridge, it can cause vortex-induced resonance. Although vortex-induced vibration is limited amplitude vibration and does not cause collapse, it can result in large displacements and discomfort to the drivers. In addition, the vortex-induced oscillations commonly occur in the low wind speed region, so the occurrence probability of vortex-induced vibration is high, resulting in long-term fatigue damage. In the previous studies, wind tunnel test is employed to investigate vortex-induced vibration. However, this technology has limitations, e.g., due to the size effect of the wind tunnel, it cannot simulate the vortex-induced vibration for a high Reynolds number; the damping of the real bridge is also difficult to simulate in the wind tunnel test. Field measurement just can overcome the limitations of the wind tunnel test, although it has some shortages, such as cost and uncontrollable wind conditions. Field monitoring provides excellent opportunities to investigate the full-scale vortex-induced vibration of bridges and the mechanism of structure and flow interaction. On the other hand, it also can validate the wind tunnel test results.

In previous research, the field monitoring for wind and wind effects on tall buildings has been comprehensively conducted [1–6]. However, the investigation of wind effects on long-span bridges based on field measurements is very rare, especially for the full-scale vortex-induced vibration. Frandsen [7] investigated the vortex-induced oscillations of the Great Belt East Bridge (one single steel box girder section) based on full-scale measurements. In that article, the wind pressure at the deck surface and accelerations were simultaneously measured. The phenomenon of cross-wind vortex-induced oscillation was observed in smooth flow, a low wind speed (around 8 m/s) and a corresponding direction perpendicular to the bridge line. The estimated full-scale

* Corresponding author. Tel.: +86 451 8628 2013; fax: +86 451 8628 2013.
E-mail address: lihui@hit.edu.cn (H. Li).

0141-0296/$ – see front matter
doi:10.1016/j.engstruct.2011.02.017

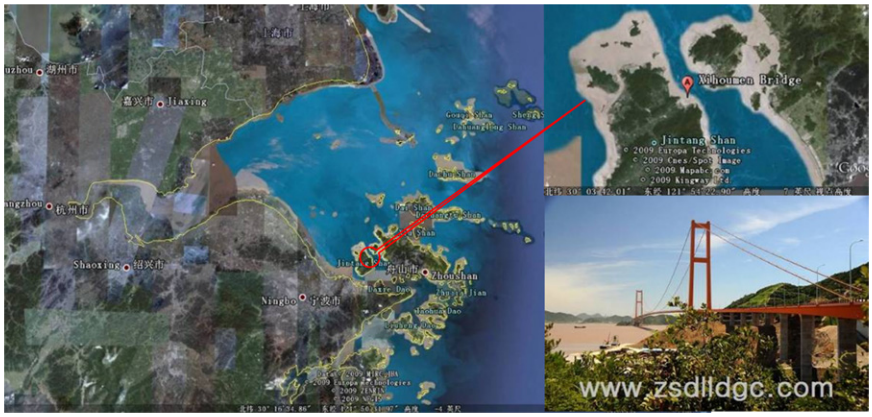

Fig. 1. Location of the investigated bridge.

Strouhal number of the deck lies in the range 0.08–0.15. According to the pressure sensors on the deck surface, the time-averaged pressure coefficients were near zero on the top flange trailing edge. Fujino and Yoshida [8] investigated the vortex-induced vibration in ten-span continuous one single steel box girder bridge section of the Tans-Tokyo Bay Crossing Bridge. The first-mode vertical vortex-induced vibration was observed with the wind directions within ±20° of the bridge transverse axis. When the wind velocity reached around 16–17 m/s, the maximum amplitude of the first-mode vertical vortex-induced vibration exceeded 50 cm. The wind tunnel tests on two-dimensional sectional models and three-dimensional bridge models were also conducted. The results of the field and wind tunnel tests were consistent with each other. To control the first and second vertical vibrations of the bridge, a new type of TMD was developed and exhibited sufficient vibration control.

With the increase in span length, twin-separated steel box girder section will be extensively used in long-span bridges to improve bridge aerodynamic stability. However, the investigations on the wind-induced vibration of this kind of bridges are insufficient so far. The investigated bridge is a suspension bridge with a main span of 1650 m. A two separated steel box girder section is employed in this bridge because both typhoon in summer and seasonal wind in winter are very strong in the site of the bridge. A sophisticated structural health monitoring (SHM) system is designed and installed on this bridge, and sensors for monitoring of wind, wind pressure and wind-induced vibration are included in the SHM system. The SHM system provides a tool to investigate the wind-induced oscillation of the prototype long-span bridge with twin-separated steel box girder and the results can be further compared with those from the wind tunnel test and the computational fluid dynamics (CFD) numerical simulation, which will aid to understanding the aerodynamic effects of this kind of bridge under different scales. Since the bridge was completed, vortex-induced vibration of this bridge has been observed and recorded by the SHM system. This paper presents the behaviour of the vortex-induced oscillation of the bridge with two separated steel box girder based on field measurement. The main objective of this study is to investigate the full-scale vortex-induced vibration of the bridge based on field measurements.

2. Description of the bridge and field measurement system

2.1. Description of the bridge

The investigated bridge is a cross-sea bridge in the East China Sea. The location of this bridge is shown in Fig. 1.

The Bridge is an asymmetric suspension bridge with a 1650 m central main span (ranking No. 2 in suspension bridges around the

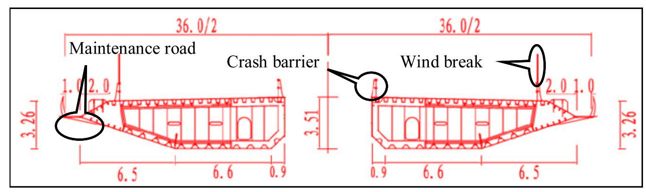

Fig. 2. Cross section of the separated box girder (unit: m).

world) and one 578 m side span. The north and south towers are made of reinforced concrete, each with a height of 236.5 m. The bridge deck is composed of two separated steel box girders with a deck centre depth of 3.51 m. The gap width between two box girders is 6 m, and the total width of the bridge deck is 36 m. The configuration of the deck is presented in Fig. 2.

2.2. Field measurement system

Typhoon and seasonal winds are very strong near this bridge, so a wind monitoring system for this bridge is set up. Two three-dimensional ultrasonic anemometers (Young Model 8100), as shown in Fig. 3(a), are installed on the east and west lighting columns at the quarter span section of the deck, and each anemometer is 6 m above the deck surface and 54.5 m above the sea surface. This type of anemometer has a good resolution (wind speed: 0.01 m/s, wind direction: 0.1°) and high accuracy (wind speed: ±1%, wind direction: ±2°), and the measurement wind speed range is (0–40 m/s). Two force-balance tri-axial accelerometers (GT02, the measured range is ±2.0 g, the sensitivity is 2.7 V/g, and the frequency band is DC ∼ 120 Hz), as shown in Fig. 3(b), are installed on the east and west sides of the bridge deck to measure the lateral, vertical and torsion accelerations of the bridge deck; the horizontal distance between them is 30 m. To obtain the wind pressure on the deck surface, 72 wind pressure sensors (CY200FA1P), as shown in Fig. 3(c), are implemented at the bridge surface at different sections, as shown in Fig. 4(a) and (b). At quarter span section S1, 52 wind pressure sensors are installed around the section, and the detailed locations of the sensors are shown in Fig. 4(c). The other 20 pressure sensors are installed at another 5 sections (S2, S3, S4, S5, S6) to investigate the span-wise correlation of the wind pressure field; each section has 4 pressure sensors, two are installed on the east side, and the other two are installed on the west side. The locations of these 5 sections are shown in Fig. 4(b). The type of wind pressure sensor is a kind of diffused silicon pressure sensor with a measured range of ±1.5 kPa, a resolution of 1 Pa, and an accuracy of ±0.25%. The frequency band is 0–1 Hz. The sensor size is 10 × 5 × 4 cm, and diameter of the gas nozzle is 8 mm. To investigate the influences